AD-A154 255 WIDE-BAND MONOLITHIC ACOUSTOELECTRIC MEMORY CORRELATORS 1/1
(U) MASSACHUSETTS INST OF TECH LEXINGTON LINCOLN LAB
R A BECKER ET AL. NOV 82 JA-5363 ESD-TR-85-089
UNCLASSIFIED F19628-80-C-0002 F/G 9/5 NL

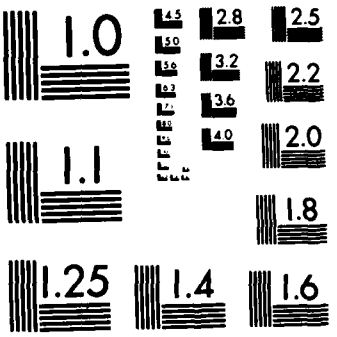

(2)

SECURITY CLASSIFICATION OF THIS PAGE (When Data Entered)

REPORT DOCUMENTATION PAGE		READ INSTRUCTIONS BEFORE COMPLETING FORM
1. REPORT NUMBER ESD-TR-85-089	2. GOVT ACCESSION NO.	3. RECIPIENT'S CATALOG NUMBER
4. TITLE (and Subtitle) Wide-Band Monolithic Acoustoelectric Memory Correlators		5. TYPE OF REPORT & PERIOD COVERED Journal Article 6. PERFORMING ORG. REPORT NUMBER JA-5363
7. AUTHOR(s) Becker, Richard A. Dr., Ralston, Richard W. Dr. Wright, Peter V.		8. CONTRACT OR GRANT NUMBER(s) F19628-80-C-0002
9. PERFORMING ORGANIZATION NAME AND ADDRESS Lincoln Laboratory, M.I.T. P.O. Box 73 Lexington, MA 02173		10. PROGRAM ELEMENT, PROJECT, TASK AREA & WORK UNIT NUMBERS 7X263304D215
11. CONTROLLING OFFICE NAME AND ADDRESS Office of the Chief of Research & Development Department of the Army, The Pentagon Washington, DC 20310		12. REPORT DATE 5 April 1982 13. NUMBER OF PAGES 10
14. MONITORING AGENCY NAME & ADDRESS (if different from Controlling Office) Electronic Systems Division Hanscom Air Force Base Bedford, MA 01730		15. SECURITY CLASS. (of this report) UNCLASSIFIED 15a. DECLASSIFICATION DOWNGRADING SCHEDULE n/a

16. DISTRIBUTION STATEMENT (of this Report)

Approved for public release; distribution unlimited.

17. DISTRIBUTION STATEMENT (of the abstract entered in Block 20, if different from Report)

18. SUPPLEMENTARY NOTES

IEEE Transactions on Sonics and Ultrasonics, Vol. SU-29, No. 6, November 1982

19. KEY WORDS (Continue on reverse side if necessary and identify by block number)

Memory correlators, Wide-band signals, Acoustic Attenuation

20. ABSTRACT (Continue on reverse side if necessary and identify by block number)

Abstract—Significant applications in radar and communication systems exist for memory correlators. These analog surface acoustic wave (SAW) devices are capable of storing one wide-band signal and then, some time later, correlating with it another wide-band signal. For some applications, these devices must be capable of handling signals with instantaneous bandwidths approaching 200 MHz. Several device types are being investigated in the surface acoustic wave memory-correlator research. Of these, the most extensively reported are the Si-$LiNbO_3$ and GaAs-$LiNbO_3$ gap-coupled types, and the ZnO-Si, ZnO-GaAs, and GaAs monolithic types. Moderate-bandwidth (60-MHz) memory correlators have been demonstrated in the $LiNbO_3$ devices and narrow-bandwidth (30-MHz) memory correlators in the ZnO devices. The purpose of this paper is to discuss the several types of monolithic memory correlators and to determine the realistic time-bandwidth limitations of each. Finally, the device design most appropriate for wide-band applications is discussed.

DD FORM 1 JAN 73 1473 EDITION OF 1 NOV 65 IS OBSOLETE

Wide-Band Monolithic Acoustoelectric Memory Correlators

RICHARD A. BECKER, MEMBER, IEEE, RICHARD W. RALSTON, AND PETER V. WRIGHT

Abstract—**Significant applications in radar and communication systems exist for memory correlators. These analog surface acoustic wave (SAW) devices are capable of storing one wide-band signal and then, some time later, correlating with it another wide-band signal. For some applications, these devices must be capable of handling signals with instantaneous bandwidths approaching 200 MHz. Several device types are being investigated in the surface acoustic wave memory-correlator research. Of these, the most extensively reported are the Si-$LiNbO_3$ and GaAs-$LiNbO_3$ gap-coupled types, and the ZnO-Si, ZnO-GaAs, and GaAs monolithic types. Moderate-bandwidth (60-MHz) memory correlators have been demonstrated in the $LiNbO_3$ devices and narrow-bandwidth (30-MHz) memory correlators in the ZnO devices. The purpose of this paper is to discuss the several types of monolithic memory correlators and to determine the realistic time-bandwidth limitations of each. Finally, the device design most appropriate for wide-band applications is discussed.**

I. Introduction

SURFACE acoustic wave (SAW) memory-correlator research has been conducted for several years [1]-[13]. Devices which exist, however, fall short of the bandwidth and dynamic-range performance demonstrated by real-time SAW convolvers. It is well known that certain signal-processing functions can be performed more efficiently in terms of size, weight, power, and cost with SAW devices than with digital systems. For example, it is the wide bandwidth (up to 200 MHz) of the SAW convolver which places it well beyond the 1984 very high-speed integrated-circuit (VHSIC) goal. Perhaps the most exciting occurrence within the ultrasonics community in the last two years has been the rapid development of the monolithic elastic SAW convolver [14]-[18]. This device is performing as well as the SAW Si-$LiNbO_3$ gap-coupled convolver [19] which has been the benchmark for comparing all programmable analog signal-processing devices. More importantly, the elastic convolver has all the advantages of a monolithic device, including reliability, ease of production and low cost.

It has long been believed that memory-correlators should yield performance equal to that of the real-time convolver as measured in terms of bandwidth, processing gain, efficiency, and dynamic range. The attractive feature of memory correlators is their ability to act as completely asynchronous programmable filters without the awkwardness of recirculating time-reversed references as required in convolvers. Monolithic memory correlators based on semiconductors can offer the possibility of integrating support electronics on the same chip. These might include amplifiers, code generators, etc. This would make for an efficient, reliable signal-processing unit with performance in terms of size, weight, power, and cost better than any current device or near-term expected device in the digital domain.

The Si-$LiNbO_3$ gap-coupled memory correlator [6] has demonstrated to date the largest bandwidth (60 MHz) and time-bandwidth product (300) of any memory correlator. The use of memory correlators would be particularly attractive if the bandwidth could be increased while extending the coherence time and maintaining adequate dynamic range in a relatively inexpensive device. For purposes of discussion in this paper, a bandwidth of 200 MHz, a coherence time of 10 μs, and a time-bandwidth product of 2000 are attractive goals to be assessed. Thus, this paper will concentrate on the monolithic technologies potentially capable of achieving wide bandwidth and wide dynamic range in a cost-effective device. These SAW device technologies include ZnO-Si, ZnO-GaAs, and GaAs. Section II will give a general understanding of how a memory correlator functions. This information is applicable to all three of the technologies being discussed. Sections III and IV will discuss ZnO devices reported in the literature. Section V will discuss GaAs devices reported in the literature as well as previously unpublished research conducted at Lincoln Laboratory, with a focus on the technology most likely to provide wideband operation.

II. Principle of Operation

All SAW memory correlators have three generic properties. They allow for the piezoelectric transduction of a SAW on the device, the storage of its associated piezoelectric potential, and the mixing of the stored potential with that of a second propagating SAW to yield the desired cross correlation of the two signals. Interdigital transducers are typically used for SAW excitation; diode arrays are most commonly used for storage; and a diode nonlinearity is usually used for mixing.

The principle of memory-correlator operation can be explained by means of the gap-coupled structure shown in Fig. 1(a). A SAW is launched from one end of the device and propagates along the $LiNbO_3$ into the region occupied by the storage medium, in this case a Si diode array. When this SAW is situated under the diode array, as shown in Fig. 1(a), the diodes are turned fully on using a current impulse. As this

Manuscript received April 5, 1982; revised August 5, 1982. This work was supported in part by the U.S. Departments of the Army and the Air Force.

The authors are with the Lincoln Laboratory, Massachusetts Institute of Technology, Lexington, MA 02173.

0018-9537/82/1100-0289$00.75

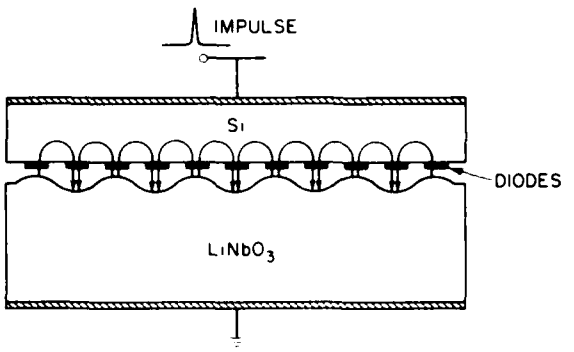

Fig. 1(a). Gap-coupled memory correlator illustrating "flash" storage technique.

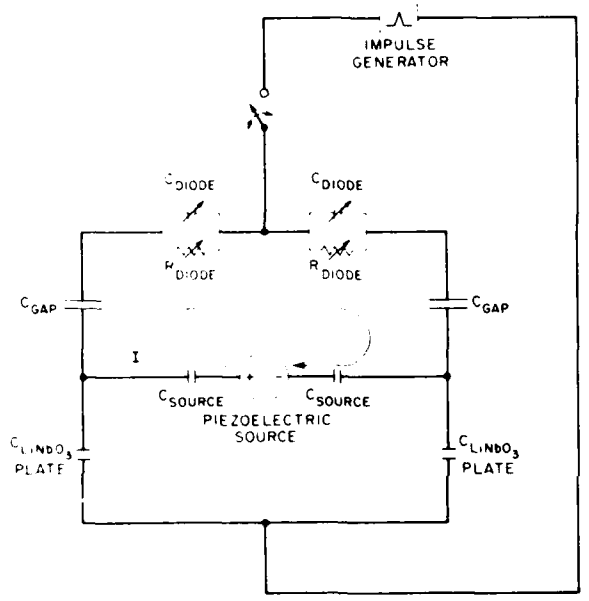

Fig. 1(b). Gap-coupled memory-correlator storage-mode equivalent circuit.

impulse terminates, all the diodes which are now heavily accumulated with majority carriers reverse bias themselves. Due to the interaction of the piezoelectric potential of the SAW and the current-rectification properties of the diodes, the charge on any given diode is composed of a spatially uniform component due to the impulse and a spatially varying component due to the SAW. If this storage process were ideally efficient, the magnitude of the stored spatially varying potential would be the same as the potential of the SAW itself.

The storage process can be understood in more detail by considering the equivalent circuit shown in Fig. 1(b). This circuit applies only during the storage operation. The piezoelectric potential of the SAW is the piezoelectric source shown in Fig. 1(b). This same source represents the spatial voltage difference between oppositely charged portions of the SAW at the $LiNbO_3$ surface below two adjacent diodes. Note that although the circuit representing only two diodes is being illustrated, the operating characteristics of the entire array can be inferred from the consideration of just two diodes. The source impedance is capacitive and is defined per unit area as

$$C_{\text{source}} = \left.\frac{D_{sc}}{\phi_{oc}}\right|_{\text{surface}}$$

where D_{sc} is the short circuit displacement and ϕ_{oc} is the open circuit potential of the SAW. The capacitance C of the $LiNbO_3$ plate is the capacitance due to the thickness of the $LiNbO_3$ itself. C_{GAP} is the capacitance produced by the air gap which separates the semiconductor from the $LiNbO_3$. Finally, the diode is represented as a parallel combination of a variable resistor R_{DIODE} and a variable capacitor C_{DIODE}. When the impulse is turned on, the majority of the spatially varying current supplied by the piezoelectric source flows through C_{GAP}, and through R_{DIODE}, which is now very small. This primary path for the current I induced by the spatially varying SAW is noted in Fig. 1(b). Simultaneously, the spatially uniform current due to the current impulse is also flowing through R_{DIODE} and C_{GAP}. As the impulse terminates, R_{DIODE} becomes very large trapping the accumulated charge on C_{DIODE}. Note that the duration of the current impulse must be appreciably less than the temporal period of the SAW being stored. This is to avoid charge smearing due to the motion of the SAW during storage. This method of storage is known as the "flash technique" and is applicable to wide-band signal storage. If now a second SAW is launched from the same end of the device in Fig. 1(a) as was the first SAW, the diode array mixes the previously stored potential with the piezoelectric potential of the propagating SAW. These local products are summed over the length of the interaction region and the result is an electromagnetic output signal which is equal to the cross correlation of the stored signal and the propagating signal. There are several other modes of operation [12]; however, none has been shown to be superior to the one discussed above.

The operation of a SAW acoustoelectric convolver without memory is often used as a benchmark in judging the performance of memory correlators. In a memory correlator, the potentials of a first SAW are stored and a second SAW mixes with the stored potentials through a semiconductor nonlinearity. However, in an acoustoelectric convolver, there is a direct mixing of the potentials of two simultaneously counterpropagating SAW's. For a given acoustoelectric device structure, transducer geometry, nonlinear mechanism, and input signal levels, the output of a convolver sets a maximum on the output level that could be obtained when the same device structure is employed for operation as a memory correlator. Equal outputs and efficiencies for the two types of devices would require that the storage mechanism yield a stored potential pattern which has the same magnitude as the piezoelectrically generated potentials of the SAW being stored. In addition, equal outputs would require that the nonlinear mixing of a second SAW with the stored potentials in a memory correlator be as efficient as the direct mixing of the potentials of two SAW's as occurs in an acoustoelectric convolver. In practice, neither of these conditions are closely approached in memory correlators, and consequently the efficiencies have been low and the dynamic ranges poor as compared to the demonstrated performance of convolvers.

The effects of dispersion and attenuation must be considered when evaluating the performance of a memory correlator, or of a similar device called a memory convolver. If a memory device with a stored SAW pattern has a second SAW launched from the opposite end of the device as the initially injected and stored SAW, then the output signal from such a device

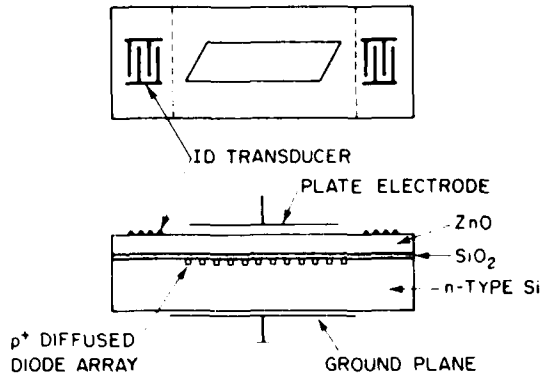

Fig. 2. ZnO-on-Si memory correlator [12]. Interdigital (ID) transducers at each end allow operation in a variety of memory correlator/convolver modes.

will be the convolution rather than the correlation of the two signals. A device operated in this way is referred to as a memory convolver. Dispersion can be a problem in devices like memory convolvers where the SAW's propagate in opposite directions. In devices where the SAW's propagate in the same direction, the effects of dispersion are the same for both signals and thus result in no distortion of the correlation. Attenuation affects both types of devices. For narrow fractional-bandwidth devices which have counterpropagating SAW's, the only effect of attenuation is a decrease in amplitude of the output signal. However, devices which have SAW's propagating in the same direction experience not only amplitude degradation but also distortion of the output correlation due to attenuation. Perhaps more serious in wide fractional-bandwidth devices are the effects of attenuation as a function of frequency. This amplitude tilt across the frequency band of interest cannot be simply corrected for signals possessing an instantaneously wide spectrum such as pseudonoise. An amplitude tilt in excess of 3 decibels is considered to be intolerable since then a substantial fraction of the information bandwidth is not being processed. Evaluation of various structures will consider these criteria.

It is important to realize that memory coorelators will be incorporated into systems only if the device dynamic range is sufficient to support the processing gain, or time-bandwidth (TB) product. The appropriate rule of thumb states that the device dynamic range must be at least 10 decibels greater than the device processing gain. For explanation of this as well as other system requirements, see [20].

III. ZnO-Si Memory Correlator

The lead research on ZnO-Si memory correlators has been conducted by Kino *et al.* at Stanford University [8]-[10], [12]. The memory correlator which they have reported on is generically shown in Fig. 2. Silicon, being nonpiezoelectric, requires an overlay of a piezoelectric material such as ZnO in order to support the desired acoustoelectric interaction. Correlators can be built which use either the first Rayleigh mode or the second Rayleigh mode, also called the Sezawa mode. The Sezawa mode has a larger piezoelectric coupling coefficient and thus has been used when a larger fractional bandwidth is desired.

Bowers *et al.* [12] recently reported the results of their Sezawa-mode memory correlator. It demonstrated a 3-decibel bandwidth of 32 MHz centered at 155 MHz ($\Delta f/f = 0.206$) and a time duration of 4 μs for a TB product of 128. The external efficiency F_{ext} was reported to be -66 dBm. Even if the fractional bandwidth can be increased to 35 percent, a center frequency of 570 MHz would be required for a 200-MHz bandwidth. Bowers *et al.* state that the absolute maximum time-bandwidth product for monolithic ZnO-Si memory correlators is 1000 due to an attenuation of 3.8 dB/μs at 300 MHz [21] and an f^2 loss dependence. It is clear from these numbers that if wide-band operation is going to be achieved, more efficient transducers, i.e., edge-bonded transducers, must be used in order to achieve large fractional bandwidths. We have shown that a $\Delta f/f$ as large as 70 percent is not unreasonable [22]. Thus a 200-MHz bandwidth device could have a center frequency as low as 285 MHz.

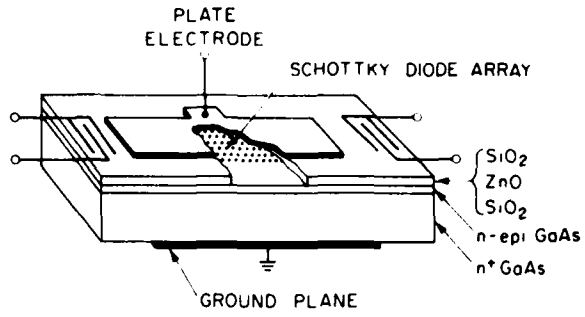

Fig. 3. ZnO-on-GaAs memory correlator [11].

The amplitude tilt across the frequency band is what will limit the performance of wide-band ZnO-Si memory correlators or convolvers. For example, a device with a bandwidth in the vicinity of 200 MHz would exhibit an amplitude tilt across that band of 4.8 dB/μs. Thus with the current ZnO technology, usable memory-correlator TB products (for $B \sim 200$ MHz) greater than 125 will not be obtained. It should be pointed out that devices with substantially lower bandwidths are possible and that improvements in the ZnO technology, which have been slow but steady in the past few years, would allow wider bandwidth devices.

IV. ZnO-GaAs Memory Correlators

The first demonstration of a ZnO-GaAs memory correlator was reported (with $B \sim 5$ MHz) by Adams *et al.* at Standard Telecommunication Laboratories [11]. A sketch of the device is shown in Fig. 3. The operation of this device is identical to that of the ZnO-Si structure. As was the case with the ZnO-Si structure, edge-bonded transducers would have to be used to achieve wide fractional bandwidth with low-insertion loss.

Just as for the ZnO-Si structure, the waveform distortion due to the amplitude tilt will limit the TB product. Since the attenuation of ZnO on GaAs is likely to be similar to that of ZnO on Si, it is reasonable to assume that the ultimate TB product (for $B = 200$ MHz) will also be similar or near 125. Thus, it does not seem possible to achieve large TB products with large bandwidths in devices which rely on lossy dispersive overlays like existing quality ZnO to support acoustoelectric interactions.

V. GaAs Memory Correlator

The use of bare GaAs has the best chance of achieving memory correlation with a TB product of 2000. Since it is both a

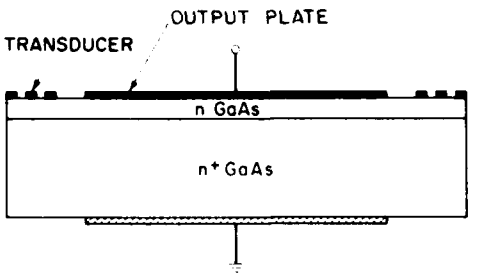

Fig. 4. Monolithic GaAs Schottky-contact convolver [24]. Both transducers and output plate are formed with Schottky contacts.

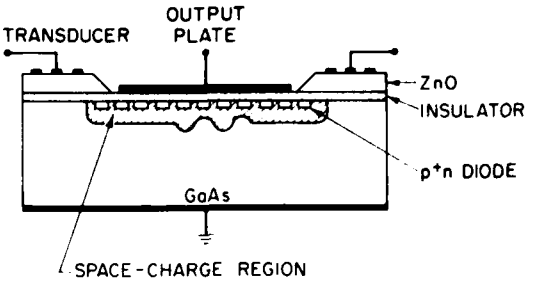

Fig. 5. In-beam GaAs memory correlator [13].

semiconductor and a piezoelectric, no lossy, dispersive ZnO overlay is required as in the case of Si. Grudkowski of the United Technologies Research Center has done most of the research on acoustoelectric devices in GaAs [24]. His work, as well as that of Loh *et al.* [13], will be discussed. Finally, previously unpublished work done at Lincoln Laboratory will be presented and a memory-correlator structure which promises to achieve the 2000 TB-product goal will be proposed.

Grudkowski's original work concerned not memory correlators, but rather monolithic GaAs convolvers of the type shown in Fig. 4. The result of this work was a demonstration of a reasonably good material nonlinear coefficient (*M* factor) and thus an efficient device. *M* factors [24] as good as -64 dBW at 165 MHz were reported on material doped at 4×10^{14} cm^{-3}. The same type of convolver was built at Lincoln Laboratory on GaAs with a doping of 1.6×10^{14} cm^{-3}. At a center frequency of 400 MHz, the peak *M* factor was measured to be -50 dBW. These convolvers utilize the nonlinearity of a reverse-biased diode formed by the output plate to achieve the mixing of the piezoelectric potentials. The optimum interaction is achieved by adjustment of the external dc bias, and is accurately calculated using Grudkowski's model.

A. In-Beam Memory Correlator

A memory-correlator structure analogous to the real-time convolver has been proposed, but not demonstrated, by Loh *et al.* [13] and is shown in Fig. 5. Here a ZnO film is used only to enhance the SAW transduction. The main difference between the GaAs memory correlator and the GaAs real-time convolvers is that the large-area Schottky contact of the convolver is replaced with very small p^+n diodes covered with an insulator and an output plate. As with the previously described GaAs convolver structures, Loh's proposed device incorporates the storage and mixing elements directly in the SAW beam path. We use the term "in beam" to describe such structures. This in-beam GaAs structure was also investigated at Lincoln Laboratory except that Schottky diodes were used rather than p^+n diodes and ZnO was not used for transduction enhancement. Both versions of this design possess a fundamental defect; that is, an inability to store a spatially varying charge pattern.

We have shown from an equivalent-circuit viewpoint the source of this defect and will indicate what device architectures alleviate the problem. To understand the problem, consider Figs. 6(a) and 6(b). Fig. 6(a) shows a monolithic memory correlator analogous to the gap-coupled memory

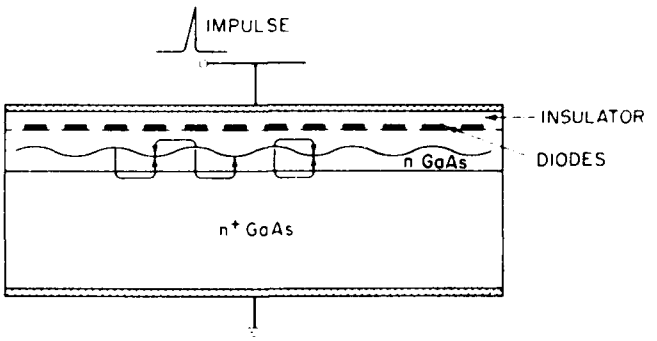

Fig. 6(a). In-beam GaAs memory correlator illustrating the failure of the "flash" storage technique.

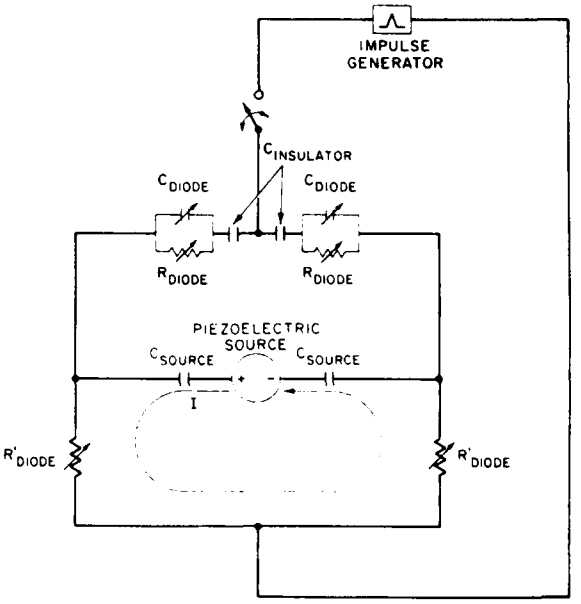

Fig. 6(b). In-beam GaAs memory-correlator storage-mode equivalent circuit.

correlator in Fig. 1(a). The spatially varying potential is at a maximum at some depth within the epilayer of Fig. 6(a). The important difference between the structures is in the current path produced by the piezoelectric SAW. Instead of flowing up through the diode contacts, as in Fig. 1(a), the majority of the spatially varying current generated by the SAW flows directly through the substrate in Fig. 6(a) to the oppositely charged portion of the SAW. The equivalent circuit shown in Fig. 6(b), which is similar to the circuit in Fig. 1(b), represents

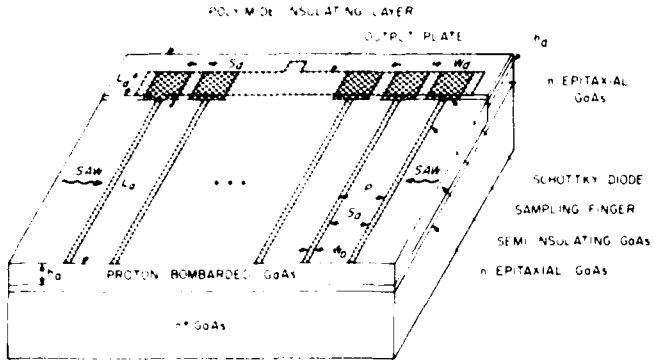

Fig. 7. Sampling-finger/Schottky-diode memory correlator.

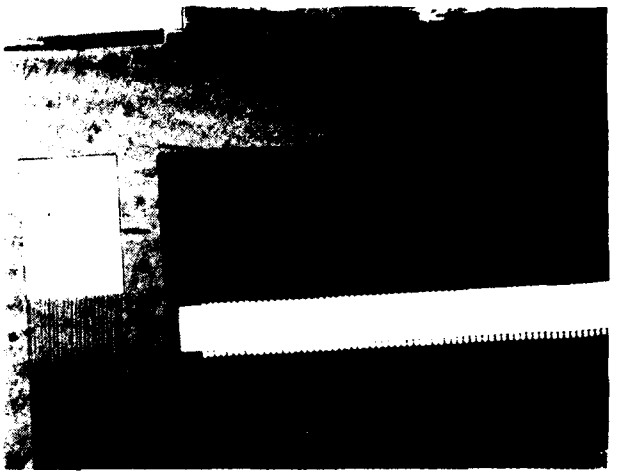

Fig. 8. Micrograph of portion of sampling-finger/Schottky-diode device: left, upper portion of input transducer; right, upper portion of segment of sampling fingers, broadened diodes, and output plate.

two adjacent diodes and, as discussed in Section II, applies to the entire array. The piezoelectric source and its source capacitance are defined the same as for the gap-coupled equivalent circuit shown in Fig. 1(b). Again the diode is represented by a variable capacitor, C_{DIODE} and a variable resistor R_{DIODE}. $C_{INSULATOR}$ is the capacitance due to the insulator between the diode contacts and the output plate. R'_{DIODE} represents the lateral resistance through the epitaxial layer and is a function of the diode depletion depth. When the current impulse is turned on, R_{DIODE} and R'_{DIODE} become small, but $R_{DIODE} >> R'_{DIODE}$, thus most of the current due to the spatially varying SAW potential flows through R'_{DIODE} as indicated by the current loop shown in Fig. 6(b). When the impulse terminates there is little piezoelectrically induced charge trapped on C_{DIODE}, whereas large amounts of spatially uniform charge due to the impulse can be stored. This is an important realization. The logical consequence is that only device architectures in which the storage interaction is physically separated from the piezoelectric medium will work well. This is because the SAW region must be piezoelectric and nonconducting. Tapped structures which satisfy this criterion are discussed below.

B. Sampling-Finger/Schottky-Diode Memory Correlator

One such device architecture attempted at Lincoln Laboratory is shown schematically in Fig. 7. It looks very similar to a tapped delay-line convolver [26], [27], but its operation is more like that of the SAW-MOSFET memory correlator reported by Smythe and Ralston [28]. This device consists of sampling fingers which occupy the same region as the acoustic waves and Schottky diodes which are outside the acoustic aperture. The acoustic region which remains piezoelectric has been proton bombarded (dose of 10^{12} cm^{-3}) to render it semi-insulating to a depth h_a. By eliminating the electron sea in the acoustic region, the piezoelectrically induced charges are imaged on the diode contacts. The sampling-finger periodicity P need only sample the spatial equivalent of the information bandwidth and not the highest SAW periodicity [28].

The sampling-finger/Schottky-diode device samples the bandwidth at a spatial frequency above the device center frequency, and can potentially support fractional bandwidths of 67 percent. Sampling-finger/Schottky-diode devices with narrow-band interdigital transducers have been fabricated and tested both as convolvers and memory correlators. A portion of one of these devices is shown in the micrograph in Fig. 8. The transducers, sampling-fingers and diodes are fabricated using Al. A spun-on polyimide layer insulates the diodes from the Al output plate. The piezoelectric potentials are sensed by the sampling fingers and then mixed in the linear diode array. For the memory device, a storage operation, as discussed in Section II, is used. Despite successful operation as a convolver, no meaningful memory correlation was observed with this structure. This disturbing result led to a more critical analysis of the device model and the realization that the previously published analysis for tapped $LiNbO_3$/metal-oxide-silicon [26] structures is, in fact, not applicable here. It is necessary to include in the model the depletion-layer capacitance of the diode array, a detail of little consequence in the earlier analysis of thin-oxide varactors. The new analysis explains the weak interaction measured in the diode device, and leads to new designs.

C. Analysis of Tapped Structures on GaAs

The first step in analyzing the sampling-finger/Schottky-diode design is determining the piezoelectric potential in the acoustic region at the surface for a given acoustic power. Note that in the case of a semiconductor, this surface potential is a function of the substrate, epilayer thickness, and the location of the depletion layer. These calculations are performed using a surface-wave layered-media computer program. For the case of the sampling-finger/Schottky-diode design, the assumptions made are shown in Fig. 9(a). The GaAs used is n/n^+. For purposes of calculation, the proton-bombarded n region is taken to be insulating and piezoelectric, whereas the residual n region and the n^+ region are assumed to be conducting and nonpiezoelectric. The piezoelectric potential and displacement at the surface can thus be calculated as a function of the bombardment depth. The potential dependence is shown in Fig. 9(b). Once the bombardment depth $h_a > \lambda/2$, the open-circuit potential approaches its maximum, implying that a bombardment depth of $\approx\lambda/2$ is sufficient to eliminate the effect of carriers below the bombardment depth and make the GaAs effectively insulating and piezoelectric.

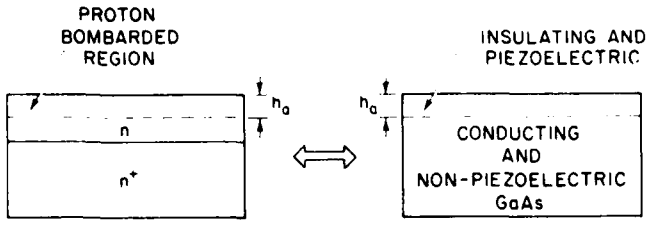

Fig. 9(a). Assumptions made in calculation of surface open-circuit potential.

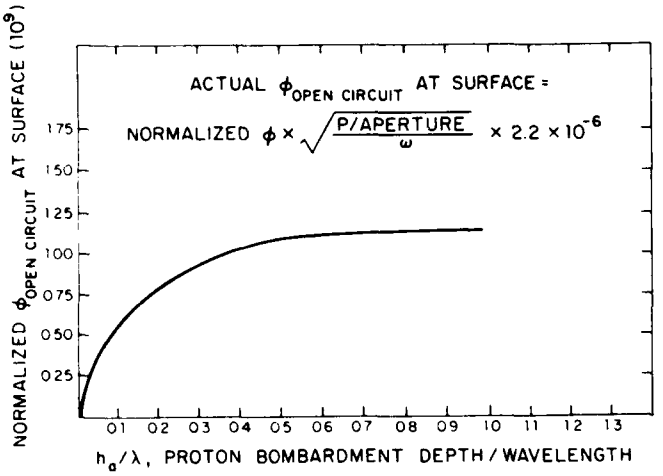

Fig. 9(b). Surface open-circuit potential versus proton-bombardment depth. Actual potential is obtained using acoustic sheet power in W/m and frequency in radians/s.

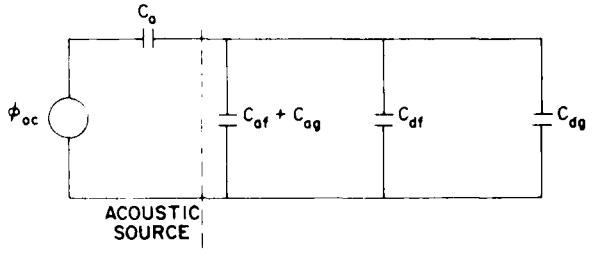

Fig. 10(a). Sampling-finger/Schottky-diode device interaction-mode equivalent circuit.

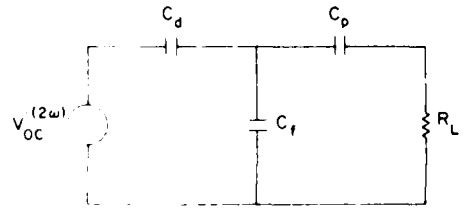

Fig. 10(b). Sampling-finger/Schottky-diode device output-mode equivalent circuit.

The surface potential and surface displacement are used to form a Thevenin equivalent source, which drives the tap/diode structure. The equivalent circuit, which adequately models the sampling-finger/Schottky-diode device, is shown in Fig. 10(a) where C_a is the acoustic source impedance, C_{af} is the finger-to-finger capacitance, C_{ag} is the capacitance from finger to ground, C_{df} is the diode-to-diode capacitance, and C_{dg} is the capacitance from diode to ground.

The source capacitance C_a is defined as

$$C_a = \frac{D_{sc} W_a L_a}{\phi_{oc}},$$

where D_{sc} is the short-circuit displacement at the surface, ϕ_{oc} is the open-circuit potential at the surface, W_a is the sampling-finger width, and L_a is the sampling-finger length, as shown in Fig. 7.

Expressions for the rest of the capacitances are derived assuming an infinite periodic finger array with a uniformly distributed charge on each sampling finger. For the desirable case of a 67 percent fractional bandwidth, at maximum permissible finger spacing, the finger pitch equals the wavelength of the highest frequency SAW. An "odd-mode" situation exists at the low edge of the band in which alternate fingers image opposite-polarity charge, an "even-mode" situation exists at the high edge of the band, and mixed modes represent the continuum within the band. Because parasitic cross-coupling is most severe for the "odd-mode" situation, it is this case which we analyze. Approximate expressions for the circuit elements are given below.

$$C_{ag} + C_{af} = \frac{L_a W_a}{P} \cdot \frac{\epsilon_s \coth(\pi h_a/P) + \epsilon_0}{[(2/\pi)^2 \cos(\pi S_a/2P)/\operatorname{sinc}(\pi W_a/2P)]} \tag{1}$$

$$C_{dg} + C_{df} = \frac{L_d W_d}{P} \cdot \frac{\epsilon_s \coth(\pi h_d/2P) + \epsilon_p \coth(\pi h_p/P)}{[(2/\pi)^2 \cos(\pi S_d/2P)/\operatorname{sinc}(\pi W_d/2P)]} \tag{2}$$

$$C_{dg} = \frac{2 L_d \epsilon_s/\sinh(\pi h_d/P)}{\operatorname{sinc}(\pi W_d/2P)} \tag{3}$$

where ϵ_o, ϵ_s, and ϵ_p are the dielectric constants of free space, the semiconductor and the piezoelectric, P is the array pitch, and the other variables and constants are defined in Fig. 7. Only the first term of each Fourier series solution has been retained.

Given the various circuit elements, one can now calculate the performance of such a device. Consider first a real-time convolution process. To calculate the strength of the mixing, we need to know the charge Q_e that is induced on C_{dg}, the diode depletion-layer capacitance, by the piezoelectric source. This is important since only charge residing in this capacitance participates in the interaction. This charge, which pumps the nonlinear capacitance, is

$$Q_e = \phi_{oc} \operatorname{sinc}(\pi W_a/2P) \left[\frac{C_{dg}}{1 + (C_{af} + C_{ag} + C_{dg} + C_{df})/C_a}\right]. \tag{4}$$

Following Grudkowski's analysis [25], the open-circuit voltage at 2ω (the mixed term) is dependent on the product of the signal and reference charges, Q_e and Q_e', or

$$V_{oc}^{(2\omega)} = \frac{Q_e Q_e'}{2\epsilon_s q N_D (P L_D)^2}. \tag{5}$$

This voltage is the source for the output circuit shown in Fig. 10(b). The elements C_d, C_f, and C_p represent, respectively,

the capacitance of the diode depletion layer, of the sampling array to ground, and of the polyimide layer. All three are simple parallel-plate capacitances because at the convolution peak, the entire depletion layer is driven in phase by the distributed 2ω generator.

For operation as a real-time convolver with a given acoustic input power, we can now calculate the output power delivered to a 50 Ω load R_L and compare theoretical and experimental efficiencies.

Devices were fabricated on epilayers with the parameters: doping density $N_D = 1.6 \times 10^{14}$ cm^{-3}, thickness $h = 11$ μm, and $N_D = 5.5 \times 10^{14}$ cm^{-3}, $h = 8.5$ μm. The proton-bombardment depths h_d were 10 μm and 7.5 μm, respectively. The most thoroughly characterized unit had the following parameters:

$F = 416$ MHz
$S_a = 10.35$ μm
$W_a = 1.15$ μm
$S_d = 2.8$ μm
$W_d = 8.7$ μm
$L_a = 730$ μm
$L_d = 100$ μm
$N_D = 5.5 \times 10^{14}$ cm^{-3}.

Amplitude tilt across the 200-MHz bandwidth of interest was was measured to be as low as 0.3 dB/μs as a GaAs delay line. The internal efficiency of this device was measured to be −71.3 dBm when operated as a convolver for a zero-bias depletion depth of 1.6 μm. This compares with a predicted efficiency of −74.8 dBm. During convolver operation, the diodes were uniformly reverse biased using an impulse. As the diodes were increasingly reverse biased, the output decreased in qualitative agreement with the theory. Storage times for this spatially uniform self-reverse bias were in the millisecond range indicating high-quality Schottky diodes.

The attractive levels of performance achieved when operating this tapped GaAs structure as a convolver suggested that the same device would work well when operated as a memory correlator. Such tests were conducted. However, no correlation output was observed. The basic problem is conflict between the requirements of efficient storage of the potentials of an initial SAW signal and efficient interaction with a subsequent SAW signal. When the device is operated so that a "snap shot" of the potentials of a SAW is efficiently stored in the device, the storage process will yield a residual spatially uniform potential which results in a depletion depth of several microns. As the carriers are pushed away from the surface, acoustoelectric interactions are weakened. Hence, the interaction of a second SAW with the stored potential pattern would be severely reduced and the device, when operated as a memory correlator, would operate well below the peak convolver efficiency. The difficulty of obtaining adequate dynamic range for operation as a memory correlator is further compounded by the presence of strong spurious outputs which are degenerate in frequency with the expected output. The deleterious effect of the depletion layer is described in more quantitative terms below.

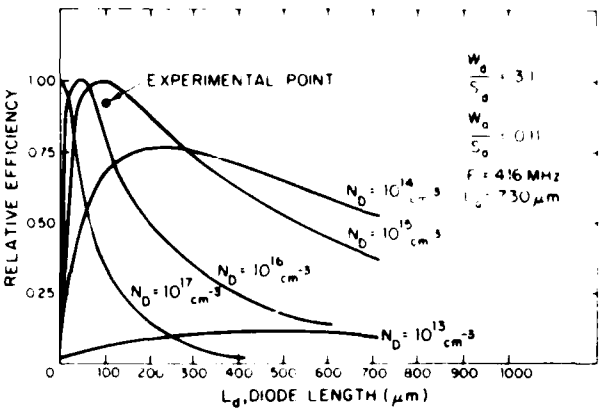

Fig. 11. Convolver efficiency relative to maximum obtainable as a function of diode length for various values of doping density in a sampling-finger/Schottky-diode device.

Consider the case of the real-time convolver. When operated in this mode, there is no storage of a SAW and therefore the increased depletion depth that would occur as a result of a storage interaction can be ignored. The circuit model of the tapped GaAs device when operated as a convolver indicates that the overall efficiency of the device can be maximized by varying the doping density N_D and the diode length L_d. Fig. 11, for example, shows the efficiency relative to the maximum obtained with this range of parameters as a function of N_D and L_d, where no spatially uniform bias is impressed on the diodes. The experimental point is plotted relative to the calculated value of the maximum obtainable efficiency. Other simulations of performance were made in which the full variety of model parameters was searched. It became clear from these simulations that it is not possible to dramatically improve the convolver efficiencies. This is in sharp contrast with projected efficiencies of similar convolvers based on Si [26]. The main reason for this is the built-in depletion layer that exists with GaAs Schottky diodes as contrasted with the near flat-band case achieved in Si-MOS devices. The concomitant weaker coupling of the SAW's to the semiconductor charges in the GaAs severely diminishes the convolver interaction.

Consider next the effect that this built-in depletion depth has on the operation of a tapped GaAs device when operated as a memory correlator. The actual depletion depth varies from the minimum as set by the built-in depth to deeper depletions caused as a result of the storage impulse. The overall efficiency of a memory correlator as a function of depletion depth is shown in Fig. 12 where the efficiencies have been normalized to the response of a device with $h_d = 0.2$ μm. While such a small depletion depth is not obtainable in GaAs devices, $h_d = 0.2$ μm is typical of Si-MOS devices. This illustrates the reason why these latter devices would generally have higher efficiencies than the particular configuration of tapped GaAs memory correlators which has been discussed up to this point.

If one assumes that a tapped GaAs device when operated as a memory correlator is biased and impulsed so as to achieve full storage of the reference charge, then the efficiency of the device as a convolver and as a memory correlator can be predicted by the same model. Thus the ability of the model to

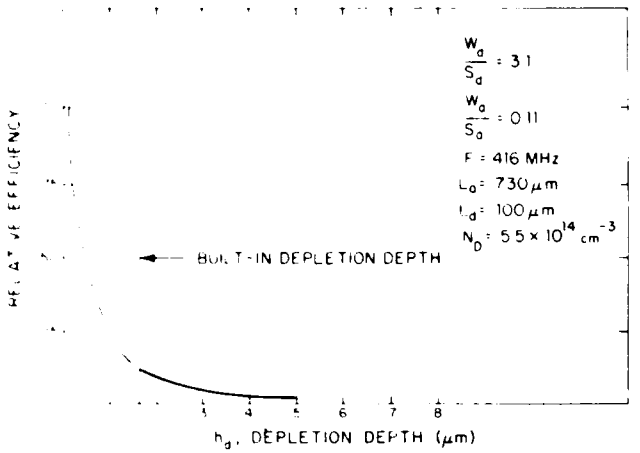

Fig. 12. Convolver efficiency relative to response at $h_d = 0.2$ μm as a function of depletion depth for sampling-finger/Schottky-diode device.

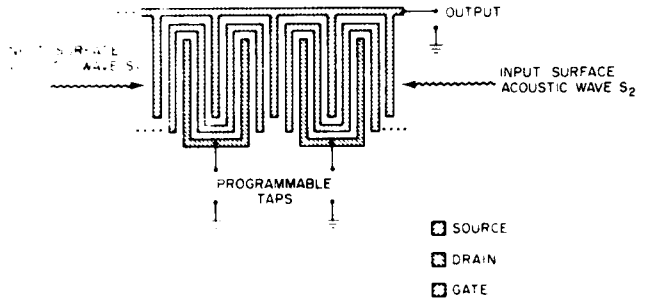

Fig. 13. Top view of tapped GaAs FET structure [24].

accurately predict the experimental convolver efficiencies lends credence to the predictions of projected memory-correlator efficiency. Assuming that edge-bonded transducers with 20-decibel insertion loss are used, an external efficiency F_{ext} of -91 dBm is predicted for optimized memory correlator operation. This will provide adequate dynamic range relative to the thermal noise floor to marginally support TB products up to 2000. An approach with more promise is described below.

D. FET Structures

Grudkowski [24] has reported a GaAs acoustoelectric device structure which uses field effect transducers (FET's) in the acoustic beam. The essential features of such a device, which has been operated as a real-time convolver, are shown in Fig. 13. Presented here is an analysis of convolver operation which serves as the first step in predicting the performance of the same structure when used as a memory correlator. The piezoelectric potentials are detected by the gates of the FET's and mixing takes place via an FET nonlinearity. Published results indicate that this design, when used as a convolver with the FET's biased in saturation, is much more efficient than the large-area Schottky-diode convolver. The analysis below explains, for the first time, this efficiency difference.

There are two nonlinearities present in the three-terminal characteristics of an FET. One is the nonlinearity between I_{GS} (gate-to-source current) and V_{GS} (gate-to-source voltage),

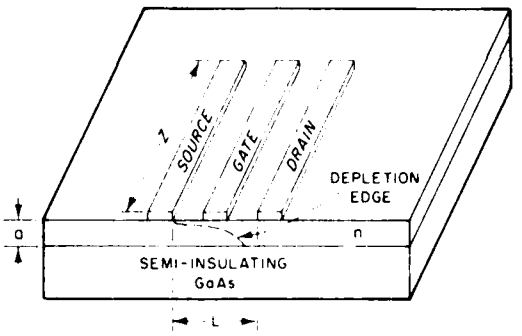

Fig. 14(a). Basic field-effect transistor.

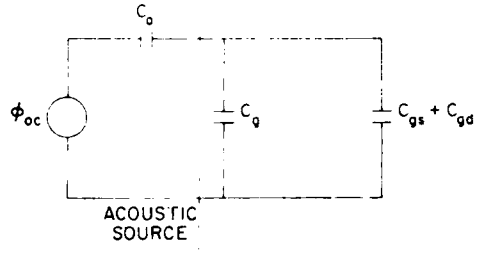

Fig. 14(b). FET convolver interaction-mode equivalent circuit.

and the other is the nonlinearity between I_{DS} (drain-to-source current) and V_{GS}. The I_{DS} (V_{GS}) nonlinearity is the dominant one since the FET is operated with the gate reverse biased [29]. It is well known that an FET in the saturation region is governed by the equation [30]

$$I_{D_{sat}} = I_p \left(1 - \frac{(V_{GS} + V_{Bi})}{V_p}\right)^2, \tag{6}$$

where

$$I_p = \frac{Z\mu q^2 N_D^2 a^3}{6\epsilon_s L},$$

$$V_p = \frac{qN_D a^2}{2\epsilon_s},$$

V_{Bi} is the built-in potential,

μ is the mobility of the electrons in the epitaxial GaAs layer, q is the charge of an electron, ϵ_s is the dielectric constant of the GaAs, and the remaining geometrical dimensions are defined in Fig. 14(a).

Writing $V_{GS} = V_{GS}(\omega = 0) + V_{GS}(\omega = \omega_a)$, one identifies the current component of interest in a real-time convolver interaction by substituting the expression for V_{GS} into (6) and expanding. The result is

$$I_{D_{sat}}(\omega = 2\omega_a) = I_p \left(\frac{V_{GS}(\omega = \omega_a)}{V_p}\right)^2. \tag{7}$$

A circuit model similar to that described for the finger/diode structure is constructed and is shown in Fig. 14(b). To determine the mixing efficiency, we have calculated the open-circuit potential ϕ_{oc} at the surface and identified

$$V_{GS}(\omega = \omega_a) = \phi_{oc} \cdot \frac{C_a}{C_a + C_g + C_{gs} + C_{gd}}. \tag{8}$$

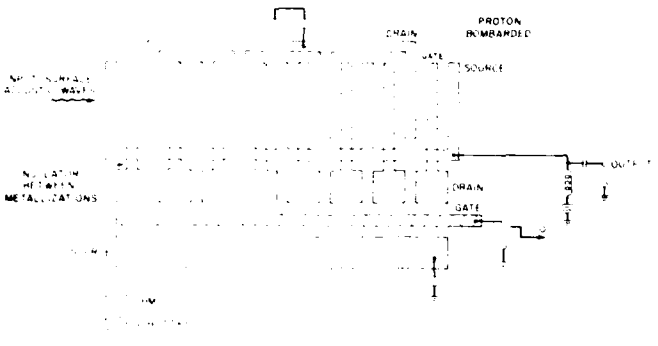

Fig. 15. Proposed tapped GaAs FET memory correlator.

where C_a is the same acoustic source impedance as in the sampling-finger/Schottky-diode case, C_g is the capacitance from the gate to the depletion-layer edge and C_{gs} and C_{gd} are the capacitances from gate-to-source and gate-to-drain, respectively. To calculate ϕ_{oc}, the following assumptions are made. As shown in Fig. 14(a), the GaAs is n/semi-insulating. We assume that the electrons in the undepleted n-region effectively screen the piezoelectrically induced charges below the depletion layer from the surface. Under this assumption of partial internal shorting of the acoustoelectric source, the calculated surface potential is the same as that given for the finger/diode in Fig. 9(b) as a function of bombardment depth.

To test our FET model, the power delivered to a 50 Ω load at pinchoff is predicted and compared with the data on convolver performance published by Grudkowski *et al.* [24]. Our model predicts a dc component of current of 2.98 mA. This compares to a value of 3 mA given in [24]. The functional dependence of the output on the $I_{DS}(\omega = 0)$ is also predicted to scale as $I_{DS}^2(\omega = 0)$ near $I_{DS}(\omega = 0) = I_{D_{sat}}$. This same functional dependence is seen in Fig. 16 of [24].

To fit our theoretical model to the measured convolver output, however, we need to use a value of $V_{GS}(\omega = \omega_a)$ which is a factor of two larger than what we calculate from (8). This disagreement is due to the over-simplified assumptions made in the calculation of ϕ_{oc}. We have assumed that the piezoelectrically induced charges below the depletion edge are totally screened from the surface. This is not completely accurate, and we see that the contribution to the surface potential from these charges will increase ϕ_{oc} and thus reduce the discrepancy between the calculated and measured $V_{GS}(\omega = \omega_a)$.

As discussed previously, real-time convolver performance sets the maximum efficiency of the same device when operated as a memory correlator. The addition of an efficient storage mechanism to the FET convolver should result in an efficient memory correlator, providing that the storage interaction does not inherently reduce the mixing action that must follow as was the case with the sampling-finger/Schottky-diode device. The addition of another array of FET's (actually one large FET switch with segmented drains), as shown in Fig. 15, would provide such a storage mechanism. To store a signal, the large FET with the segmented drains is rapidly turned off when the SAW lies underneath the gates of the FET taps which span the acoustic aperture. This is the same storage technique demonstrated by Smythe and Ralston [28] in a $Si/LiNbO_3$, SAW/charge-coupled device. Through such a storage mechanism, an image of the piezoelectric charge distribution is trapped on the gates of the FET's in the acoustic aperture. Subsequently, this stored charge pattern interacts with a second SAW through the same FET nonlinearity described above for the case of the convolver.

Design issues to be considered for the proposed memory-correlator device include: fabrication constraints, power dissipation and transconductance of the FET taps, and the channel conductance of the FET switch in both "on" and "off" states. Since now each tap requires an FET rather than just a sampling finger, the photolithography requirements are more stringent. However, a device with a 200-MHz bandwidth requires about 1-μm-wide lines and spaces, a resolution within the capability of conventional photolithography.

One must also be concerned with the power dissipation of a structure that contains many FET's in close proximity. As seen from (7), the way to increase $I_{D_{sat}}(\omega = 2\omega_a)$ is to increase I_p by design [30]. However, increasing I_p increases $I_{D_{sat}}(\omega = 0)$ and thus, since one memory correlator contains at least 2 TB of these FET taps, the dc power dissipation with high-I_p FET's would be prohibitive. Because $I_{D_{sat}}(\omega = 2\omega_a)$ is not a function of $V_{GS}(\omega = 0)$, there is a way to avoid this power-dissipation problem. The FET taps can be made with as large an I_p as required and then uniformly biased to reduce $I_{DS}(\omega = 0)$ to as small a value as desired.

The transconductance of the FET taps must be large enough so that the cutoff frequency of the FET's is greater than the acoustic frequency. Special attention must be paid to the calculation of the transconductance since the drains and sources have an appreciable contact resistance due to their small lengths. Taking this into account, one finds that the predicted cutoff frequency is still well beyond the acoustic frequencies required to yield a 200-MHz bandwidth. Finally, the channel conductance of the FET switch must be able to be made very small in a time short compared to the SAW period. Thus the gate capacitance must be small and the leakage currents, both source to gate and source to drain, must be small enough to allow a reasonable storage time. The gate capacitance poses no problem in terms of rapid turnoff. To determine the leakage currents in an "off-state" FET, several FET's fabricated at Lincoln Laboratory were tested. The ratio of the on-state channel conductance to the off-state channel conductance was found to be 10^7, indicating milliseconds of storage time. Since these test FET's were not optimized for a memory-correlator application, it is felt that this ratio can be improved further.

On the basis of published data on FET convolver performance and the analysis and tests reported here, we predict that a tapped FET memory correlator using edge-bonded transducers for wide fractional bandwidths could yield useful efficiency and dynamic range in a device having a TB product of 2000 with a 200-MHz bandwidth. This proposed structure is shown schematically in Fig. 15.

VI. Conclusion

A review of memory correlator research indicates that a memory correlator with a TB product of 2000 (for $B \sim 200$ MHz) is not likely to result from existing configurations. The main problem with the ZnO-Si or ZnO-GaAs technologies is

the acoustic attenuation due to the ZnO film. This attenuation leads to an unacceptable signal distortion as well as a reduction of the device dynamic range and thus a loss in processing gain. We have concluded that new approaches must be taken. One of these approaches, the GaAs sampling-finger/Schottky-diode design, does not result in a sufficiently strong acoustoelectric interaction due mainly to the large built-in depletion layer of the diode array. A more complex structure, a GaAs FET memory correlator, has been proposed. Preliminary measurements along with theoretical projections indicate that this design promises to achieve time-bandwidth products of 2000 with bandwidths of 200 MHz.

Acknowledgment

The authors would like to acknowledge C. Bozler and K. Nichols for the GaAs epitaxial layers used for device fabrication, L. Lowe and A. Smith of the Rome Air Development Center Radiation Facility, Hanscom A.F.B., MA for the high-energy proton bombardment, E. Adler of McGill University for calculations using the surface acoustic wave layered-media computer program, G. Hansell for the GaAs FET's, J. Cafarella, R. Murphy, S. Reible, E. Stern, and R. Withers for many helpful discussions, J. Holtham for computer programming, R. Williamson for his critical reading of the manuscript and many helpful suggestions, and members of the Analog Device Technology Group who aided in fabrication and testing.

References

[1] A. G. Bert, B. Epstein, and G. Kantorowicz, "Charge storage of acoustic RF signals," *Appl. Phys. Lett.*, vol. 21, pp. 50–52, 1972.

[2] E. Stern and R. C. Williamson, "New adaptive-signal-processing concept," *Electron. Lett.*, vol. 10, pp. 58–59, 1974.

[3] A. Bers and J. H. Cafarella, "Surface wave correlator-convolver with memory," in *1974 Ultrasonics Symp. Proc.*, pp. 778–787, New York: IEEE, 1974.

[4] Ph. Defranould, H. Gautier, C. Maerfeld, and P. Tournois, "*P-N* diode memory correlator," in *1976 Ultrasonics Symp. Proc.*, pp. 336–347, New York: IEEE, 1976.

[5] R. W. Ralston, J. H. Cafarella, S. A. Reible, and E. Stern, "Improved acoustoelectric Schottky-diode/$LiNbO_3$ memory correlator," in *1977 Ultrasonics Symp. Proc.*, pp. 472–477, New York: IEEE, 1977.

[6] D. H. Hurlburt, R. W. Ralston, R. P. Baker, and E. Stern, "An acoustoelectric Schottky-diode memory-correlator subsystem," in *1978 Ultrasonics Symp. Proc.*, pp. 33–37, New York: IEEE, 1978.

[7] H. Gautier, C. Maerfeld, and P. Tournois, "Acoustic memory correlator using GaAs Schottky diodes," *Appl. Phys. Lett.*, vol. 32, pp. 517–518, 1978.

[8] G. S. Kino, "Zinc oxide on silicon acoustoelectric devices," in *1979 Ultrasonics Symp. Proc.*, pp. 900–910, New York: IEEE, 1979.

[9] H. C. Tuan, J. E. Bowers, and G. S. Kino, "Theoretical and experimental results for monolithic memory correlators," *IEEE Trans. Sonics Ultrason.*, vol. SU-27, pp. 360–369, 1980.

[10] R. L. Thornton and G. S. Kino, "Monolithic ZnO on Si Schottky diode storage correlator," in *1980 Ultrasonics Symp. Proc.*, pp. 124–128, New York: IEEE, 1980.

[11] G. R. Adams, J. D. Jackson, and J. S. Heeks, "Monolithic ZnO-GaAs acousto-electric devices," in *1980 Ultrasonics Symp. Proc.*, pp. 109–112, New York: IEEE, 1980.

[12] J. E. Bowers, B. T. Khuri-Yakub, and G. S. Kino, "Monolithic Sezawa wave storage correlators and convolvers," in *1980 Ultrasonics Symp. Proc.*, pp. 118–123, New York: IEEE, 1980.

[13] K. W. Loh, D. K. Schroder, and R. C. Clarke, "The GaAs SAW diode storage correlator," in *1980 Ultrasonics Symp. Proc.*, pp. 98–103, New York: IEEE, 1980.

[14] H. Gautier and C. Maerfeld, "Wideband elastic convolvers," in *1980 Ultrasonics Symp. Proc.*, pp. 30–36, New York: IEEE, 1980.

[15] I. Yao, "High performance elastic convolver with parabolic horns," in *1980 Ultrasonics Symp. Proc.*, pp. 37–42, New York: IEEE, 1980.

[16] B. J. Darby, D. Gunton, and M. F. Lewis, "The design and performance of a small efficient SAW convolver," *1980 Ultrasonics Symp. Proc.*, pp. 53–58, New York: IEEE, 1980.

[17] K. L. Davis and J. F. Weller, "Elastic convolver using planar prism waveguide couplers," in *1980 Ultrasonics Symp. Proc.*, pp. 74–76, New York: IEEE, 1980.

[18] Pierre A. Dufilie, "Low cost SAW convolver with high spurious suppression," in *1980 Ultrasonics Symp. Proc.*, pp. 43–47, New York: IEEE, 1980.

[19] S. A. Reible, "Acoustoelectric convolver technology for spread-spectrum communication," *IEEE Trans. Sonics Ultrason.*, vol. SU-28, pp. 185–195, 1981.

[20] J. H. Cafarella, "Device requirements for spread-spectrum communications," *SPIE Proc.*, vol. 209, pp. 53–56, 1979.

[21] J. deKlerk, R. W. Weinert, and B. R. McAvoy, "SAW attenuation in hydrothermally grown ZnO," in *1978 Ultrasonics Symp. Proc.*, pp. 667–669, New York: IEEE, 1978.

[22] D. E. Oates and R. A. Becker, "$LiNbO_3$ surface-acoustic-wave edge-bonded transducers on ST quartz and (001)-cut GaAs," in *1980 Ultrasonics Symp. Proc.*, pp. 367–370, New York: IEEE, 1980.

[23] E. L. Adler and J. H. Cafarella, "The effect of acoustic dispersion and attenuation on SAW convolver performance," in *1980 Ultrasonics Symp. Proc.*, pp. 1–4, New York: IEEE, 1980.

[24] T. W. Grudkowski, G. K. Montress, M. Gilden, and J. F. Black, "GaAs monolithic SAW devices for signal processing and frequency control," in *1980 Ultrasonics Symp. Proc.*, pp. 88–97, New York: IEEE, 1980.

[25] T. W. Grudkowski, "Active acoustic waves and electrons in GaAs," Microwave Laboratory Rep. 2440, W. W. Hansen Laboratories of Physics, Stanford Univ., May 1978.

[26] G. S. Kino and W. R. Shreve, "Theory of strip coupled acoustic devices," *J. Appl. Phys.*, vol. 44, pp. 3960–3966, 1973.

[27] L. R. Adkins, "Strip coupled AlN and Si on sapphire convolvers," in *1973 Ultrasonics Symp. Proc.*, pp. 148–151, New York: IEEE, 1973.

[28] D. L. Smythe and R. W. Ralston, "A surface-acoustic-wave/metal-oxide-silicon field-effect transistor memory correlator," *Appl. Phys. Lett.*, vol. 38, pp. 886–887, 1981.

[29] (An alternate way to view the nonlinearity in the case of a SAW device is to consider the charge density associated with the SAW as modulating the semiconductor doping density and depletion edge) R. Withers, Lincoln Laboratory, M.I.T., private communication.

[30] S. Sze, *Physics of Semiconductor Devices*. New York: John Wiley and Sons, 1969.

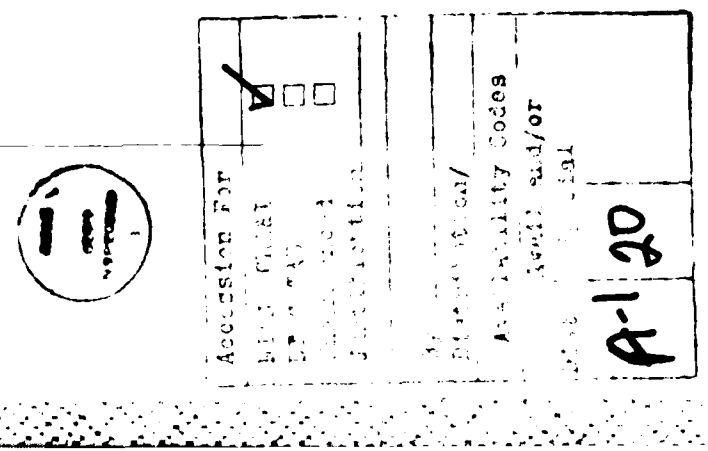

END

FILMED

7-85

DTIC